JOURNAL OF GEOPHYSICAL RESEARCH: OCEANS, VOL. 118, 3350–3369, doi:10.1002/jgrc.20248, 2013

Implications from the comparisons between two- and three-dimensional model simulations of the Hurricane Ike storm surge

Lianyuan Zheng,[1] Robert H. Weisberg,[1] Yong Huang,[1] Rick A. Luettich,[2] Joannes J. Westerink,[3] Patrick C. Kerr,[3] Aaron S. Donahue,[3] Gary Crane,[4] and Linda Akli[4]

Received 15 February 2013; revised 30 April 2013; accepted 20 May 2013; published 11 July 2013.

[1] We apply the Finite Volume Coastal Ocean Model to simulate the Hurricane Ike storm surge using two-dimensional (2-D) and three-dimensional (3-D) formulations. The high resolution, unstructured grid extends over the Gulf of Mexico with open boundaries in the Straits of Florida and the Yucatan Channel. With the same wind and pressure forcing, the bottom drag coefficients for the baseline 2-D and 3-D simulations are determined by spatially varying Manning coefficients and constant bottom roughness, respectively. The baseline 2-D model simulates both the forerunner and the surge, whereas the baseline 3-D model simulates the surge, but underestimates the forerunner. Increasing the minimum Manning coefficient reduces the 2-D forerunner and the surge. Manning coefficient and bottom roughness parameterizations produce different bottom drag coefficients. Using the same bottom drag coefficient, the 2-D simulation yields a smaller surge than in three dimensions. This is investigated for scenarios of either constant or variable bottom roughness where the bottom roughness is determined through Manning coefficient transformation. These sensitivity studies indicate that storm surges, simulated either in two dimensions or three dimensions, depend critically upon the parameterizations and the parameter values used for specifying bottom stress (and similar may be said of surface stress). Given suitable calibration, 2-D and 3-D models may adequately simulate storm surge. However, it is unclear that a calibration for a given storm and location may apply generally. Hence additional experimental guidance is required on the parameterizations and the parameter values used for both the surface and bottom stresses under severe wind conditions.

Citation: Zheng, L., R. H. Weisberg, Y. Huang, R. A. Luettich, J. J. Westerink, P. C. Kerr, A. S. Donahue, G. Crane, and L. Akli, Implications from the comparisons between two- and three-dimensional model simulations of the Hurricane Ike storm surge, *J. Geophys. Res. Oceans*, *118*, 3350–3369, doi:10.1002/jgrc.20248.

1. Introduction

[2] Hurricanes are defined as tropical cyclones with wind speeds exceeding 74 miles per hour. Those in the Gulf of Mexico may originate in the tropical Atlantic Ocean, the Caribbean Sea or locally in the Gulf of Mexico itself. Depending on their intensity, size, orientation, speed of approach and point of landfall, such hurricanes may cause significant losses of life and property throughout North and Central America. For instance, the two successively active years of 2004 and 2005, with Hurricanes Charley, Frances, Ivan, and Jeanne in 2004 and Dennis, Katrina, Rita, and Wilma in 2005, exacted 1000s of lives and 100s of billions of dollars in economic loses to housing, commerce, municipalities, infrastructure, forests, agriculture, and coastal ecosystem services [e.g., *Hagy et al*., 2006; *Sallenger et al*., 2006]. Hurricane Ike in 2008 added further dislocations and loses. Of the various causal agents of damage, excepting the highest wind category storms (e.g., Hurricane Andrew in 1992), it is generally the inundation by hurricane storm surge and waves that prove to be the most deadly and costly of these.

[3] Storm surge is defined as the abnormal change in sea level that may accompany either extratropical or tropical storms. Such storm surge is in addition to the tides, and its magnitude depends on the wind speed, the storm size (often defined by the radius to maximum winds), the storm track (and hence point of landfall), the speed of translation, the direction from which the storm makes landfall, its central pressure, the width and slope of the adjacent continental shelf and the local land topography [e.g., *Weisberg and Zheng*, 2006a]. A storm surge, in essence, derives primarily from the slope of the sea surface that sets up to balance the Coriolis force and the difference between the wind stress on the sea surface and the bottom stress due to the water

[1]College of Marine Science, University of South Florida, Florida, USA.
[2]Institute of Marine Sciences, University of North Carolina at Chapel Hill, North Carolina, USA.
[3]Department of Civil and Environmental Engineering and Earth Sciences, University of Notre Dame, Indiana, USA.
[4]Southeastern Universities Research Association, Washington, D. C.

Corresponding author: L. Zheng, College of Marine Science, University of South Florida, FL 33701, USA. (lzheng@marine.usf.edu)

©2013. American Geophysical Union. All Rights Reserved.
2169-9275/13/10.1002/jgrc.20248

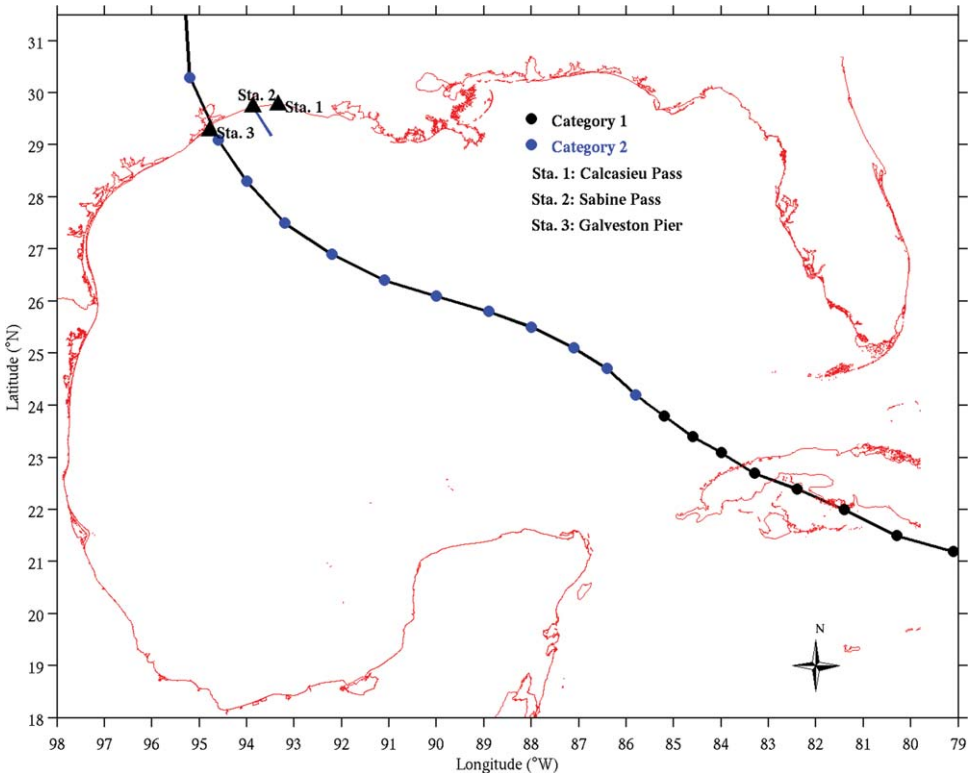

Figure 1. Hurricane Ike track and intensity. The filled triangles are three tide gauged stations (Calcasieu Pass, Sabine Pass, and Galveston Pier) where the observed and simulated storm surges are compared. The across-shore line is chosen for the momentum balance analyses.

motion caused by the wind stress. The Coriolis force is particularly important in deep water, but becomes of lesser importance in shallow water as the bottom friction increases. Thus, the initial phase of the storm surge includes a forerunner due to an Ekman-geostrophic adjustment to alongshore wind stress [e.g., *Weisberg et al*., 2000], whereas the mature phase is primarily associated with pressure gradient (due to the sea surface slope) tending to balance the difference between the surface and bottom stresses.

[4] Given the geometrical complexities of the shoreline, the bottom topography and the land elevations (in addition to the sensitivity of the surge to specific storm characteristics), accurate simulations of hurricane storm surge, and the accompanying waves require three elements. The first is a numerical circulation model that is complete enough in its physical formulation and has resolution sufficient to account for the important conveyances of mass. The second is an accurate set of bathymetric and topographic data on which to overlay the numerical model grid. The third is atmospheric forcing data of sufficient accuracy to portray the conditions of the storm for which the surge and waves are to be simulated. Given these three elements, any model simulation will also be sensitive to the specifications of the surface and bottom stresses (i.e., the parameterizations and the parameter values that are used).

[5] The model used herein is the Finite Volume Coastal Ocean Model (FVCOM), introduced by *Chen et al*. [2003]. As a primitive equation, unstructured grid model, its physics are complete enough, and it may be employed with very high resolution where needed. It may also be run as a vertically integrated, two-dimensional (2-D) model or in its fully three-dimensional (3-D) form. This attribute is important for the present study because the bottom stress parameterizations in either the 2-D or 3-D formulations may differ, and the ramifications of these differences are what we endeavor to investigate. Thus, we use the wind stress parameterization provided by P. C. Kerr et al. (U.S. IOOS Coastal & Ocean Modeling Testbed: Inter-Model Evaluation of tides, waves, and hurricane surge in the Gulf of Mexico, submitted to *Journal of Geophysical Research: Oceans*, 2013), posited as the most accurate of the Hurricane Ike wind stress renditions, and concentrate on the surge effects caused by different bottom stress parameterizations, and, in particular, how these vary under 2-D and 3-D model formulations. For a detailed description of Hurricane Ike and its wind and pressure fields, we refer to Kerr et al. (submitted manuscript, 2013). Figure 1 shows the Hurricane Ike storm track and intensity variations from 10 September to 13 September 2008, as it moved over Cuba, entered the Gulf of Mexico and proceeded toward landfall near Galveston TX (data downloaded from National Hurricane Center website "http://www.nhc.noaa.gov/").

[6] Our study of Hurricane Ike builds on a previous comparison between storm surges under 2-D and 3-D formulations by *Weisberg and Zheng* [2008], who used FVCOM to investigate the potential (hypothetical) storm surge that could have befell the Tampa Bay region had Hurricane Ivan made landfall there instead of near the Florida/Alabama border. That study, in which the same bottom drag coefficient was used for both 2-D and 3-D simulations,

found larger surge heights under the 3-D formulation. The explanation had to do with the horizontal velocity structure with depth and hence the magnitude of the bottom stress. With the 2-D simulated depth-averaged velocity being larger than the 3-D simulated near bottom velocity, the 2-D model formulation generated a larger bottom stress than the 3-D model formulation. As a result, the simulated surface slope was smaller for the 2-D simulation, and its spatially integrated values (the storm surges at any location) were therefore smaller.

[7] The intent of this aforementioned study was to compare the consequences of model formulation (2-D versus 3-D) with all else kept as similar as possible. However, it does not necessarily follow that the drag coefficients under 2-D and 3-D simulations should be the same. With model simplification come increased dependence on parameterizations, and a 2-D formulation is a simplification over a 3-D formulation. To investigate the potential for parameters to alter simulation results we consider four different approaches. The first (our baseline simulation) compares 2-D results using spatially varying Manning coefficients with 3-D results using constant bottom roughness. The second compares 2-D results with two different values of Manning coefficient minima. The third (similar to *Weisberg and Zheng* [2008]) compares 2-D and 3-D results with similar bottom drag coefficients. The fourth compares 2-D and 3-D results with the 3-D simulation using variable bottom roughness derived from the Manning coefficients used in the 2-D formulation. Hence the present study (as applied to Hurricane Ike) will explore how different formulations for the bottom drag coefficients in 2-D and 3-D ocean models may affect the storm surge simulations under the same surface forcing and model grid configurations.

[8] This paper is organized as following. Section 2 discusses the bottom friction parameterizations for 2-D and 3-D model simulations. Section 3 defines the model configurations used in this study. Section 4 then compares the 2-D and 3-D Hurricane Ike storm surge simulations including tides, compares results with and without wave effects and diagnoses the physical balances that account for the 2-D and 3-D simulation differences under the first scenario mentioned above. Given the differences observed, section 5 further examines the effects of the bottom stress parameterizations and parameter values on the simulated storm surge. A discussion and conclusions follow in section 6.

2. Bottom Friction Formulations and Parameterizations for 2-D and 3-D Models

[9] For use in the momentum equations, the bottom friction follows a quadratic drag law expressed as:

$$\vec{\tau}_b = \rho_0 \cdot C_d \cdot |\vec{V}_b| \cdot \vec{V}_b \tag{1}$$

where $\vec{\tau}_b$ is the bottom (friction) stress, ρ_0 is the water density, $\vec{V}_b$ is the velocity vector (either the depth-averaged velocity vector for a 2-D model, or the near bottom velocity vector for a 3-D model) and C_d is the drag coefficient. In a 2-D model, the C_d may be expressed as a function of a Manning coefficient (n) and the total water depth ($H = h + \zeta$, where h is water depth and ζ is sea level, both referenced to mean sea level) by the following equation:

$$C_d = g \cdot n^2 / H^{1/3} \tag{2}$$

[10] For coastal waters (continental shelves and estuaries), studies suggest Manning coefficients that are spatially varying within a range of 0.02–0.045 [e.g., *Bunya et al*., 2010]. In 3-D models, the C_d is generally determined by scaling to account for the fact that the magnitude of the horizontal velocity vector varies in accordance with a logarithmic bottom boundary layer, thus:

$$C_d = \max\left[\kappa^2 / \ln\left(\frac{z_{ab}}{z_0}\right)^2, 0.0025\right] \tag{3}$$

where κ is the von Karman constant ($\kappa = 0.4$), z_0 is the bottom roughness parameter that is related to the seabed structure and z_{ab} is the height of the model's vertical grid point that is closest to the bottom. Similar to the specification of a Manning coefficient, the bottom roughness may also be spatially varying with a typical (two order of magnitude) range of from 0.1 cm to a few centimeters [e.g., *Feddersen et al*., 2003].

[11] How the respective C_d's vary as a function of water depth and either Manning coefficient or bottom roughness are shown in Figure 2 [based on the equations (2) and (3)]. The top plot is for 2-D formulation, and the bottom plot is for 3-D formulation. Using typical values for n and z_o, the bottom friction drag coefficients under 2-D and 3-D formulations differ by an order of magnitude. We note that for the 3-D case we are using 11 uniformly distributed σ-layers in the vertical. Also, at this stage in our presentation, while there an order-of-magnitude difference in the bottom drag coefficients between 2-D and 3-D formulations it is premature to translate this finding to differences in bottom stress because of the quadratic drag law. This step must await the calculation of the horizontal velocity as we will see in section 4.

3. Model Configuration

[12] Here we use FVCOM version 3.1 with MPI parallelized coding and high computation and I/O efficiency NetCDF input/output writers. FVCOM is a 3-D, time- and density-dependent, prognostic numerical ocean circulation model that employs an unstructured triangular grid in the horizontal and a terrain-following σ-coordinate in the vertical. Such grid is capable of accurately matching complicated coastal geometries and bathymetries and with flooding and drying can also include complex land topographies. The flexibility of unstructured grids also facilitates the increase of resolution where needed. For turbulence closure, the FVCOM utilizes the *Mellor and Yamada* [1982] level-2.5 turbulence closure submodel, as modified by *Galperin et al*. [1988] for flow-dependent vertical mixing coefficients, and the *Smagorinsky* [1963] formulation for calculating the horizontal mixing coefficients. The equations of motion are solved by a finite volume computational method of second-order accuracy, which conserves water properties (mass, energy, salt, and heat) over long simulations. Wetting and drying, an important component for inundation simulations [e.g., *Zheng et al*., 2003], is incorporated in the model.

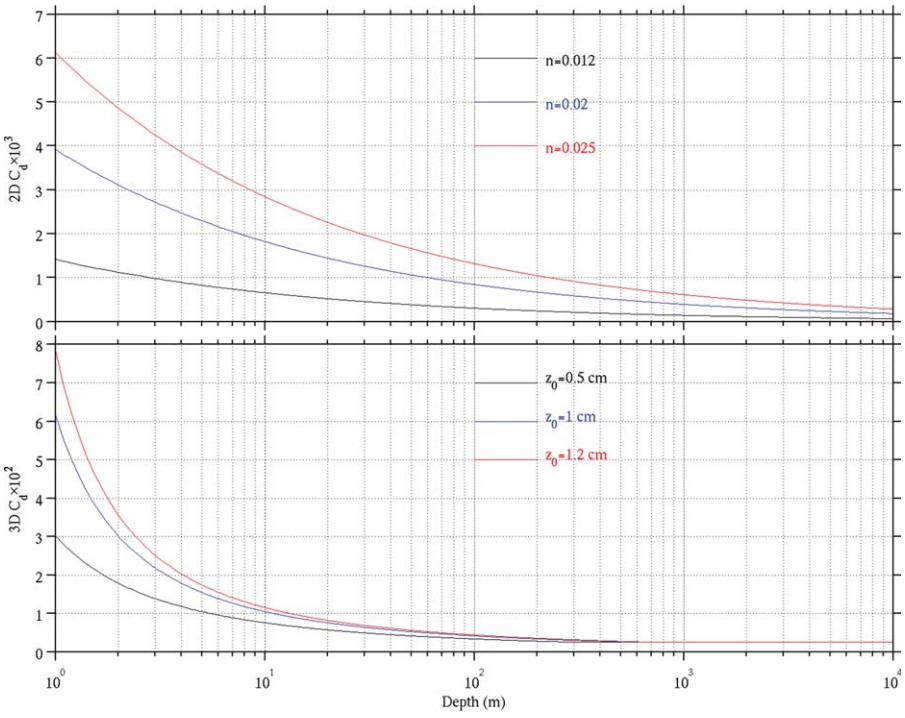

Figure 2. Bottom drag coefficient varied with water depth for the (top) 2-D formulation defined by equation (2) and (bottom) 3-D formulation defined by equation (3).

[13] Beginning with its inception [*Chen et al*., 2003], FVCOM has gained broad applications to estuaries [e.g., *Chen et al*., 2008b; *Weisberg and Zheng*, 2006b; *Zheng and Weisberg*, 2010], the continental shelf [e.g., *Chen et al*., 2008a; *Rego and Li*, 2010; *Weisberg et al*., 2009; *Zheng and Weisberg*, 2012], and the deep ocean [e.g., *Chen et al*. 2009]. Prior to using the present surface forcing products for Hurricane Ike, applications of FVCOM to simulating hurricane storm surges employed either the prototypical and symmetrical hurricane wind and pressure fields of *Holland* [1980] [e.g., *Weisberg and Zheng*, 2006a, 2006c] or the hypothetical use of wind products as in the Hurricane Ivan-like case applied to Tampa Bay by *Weisberg and Zheng* [2008].

[14] The numerical wave model used in this study is the unstructured, triangular grid version of the third generation Simulating WAves Nearshore (SWAN), or unSWAN, as described by *Zijlema* [2010]. Coupling with surge was via wave radiation stress, as described by *Huang et al*. [2010] in application to the Hurricane Ivan-like simulation for Tampa Bay.

[15] Requirements on the storm surge model grid configuration include a model domain that: (a) is large enough to both contain the storm and to minimize open boundary effects [e.g., *Orton et al*., 2012]; (b) extends landward to include the entire region of potential inundation; and (c) has a model grid with resolution high enough to include the geometric details of the region of potential inundation. The model grid used in this Hurricane Ike application is shown in Figure 3. It has 417,642 triangular nodes and 826,866 nonoverlapping triangular cells. The higher resolution grids are located in Galveston Bay, Texas where Hurricane Ike made landfall and in the Mississippi River Delta region characterized by multiple river channels and narrow creeks. Grid sizes range from 100 m in the coastal inundation region to about 30 km in the deep ocean interior region (Figure 4). The model domain has two open boundaries located in the Straits of Florida and the Yucatan Channel, both of which are more than 1000 km distant from the Hurricane Ike landfall near Galveston Bay, Texas. For the 3-D model simulations, we employed 11 uniform terrain following σ-layers in the vertical.

[16] Prior to simulating the storm surges, we tested the model simulations of tides in either two dimensions or three dimensions (including the propagation through the open boundaries and the equilibrium forcing in the Gulf of Mexico of the eight principal tidal constituents: M_2, S_2, N_2, K_2, O_1, K_1, P_1, and Q_1). Detailed comparisons between the 2-D and 3-D model simulations of tides, when quantitatively gauged against observations from 59 National Oceanic and Atmospheric Administration (NOAA) tide gauge stations, are presented in Kerr et al. (submitted manuscript, 2013). These tidal constituent results were generally found to be good, particularly for the semidiurnal species, and the tidal simulations were found to be relatively insensitive to either the formulations in two and three dimensions or to the parameterizations of bottom stress.

[17] For the storm surge simulations, the model was driven by wind stress and atmospheric pressure gradient acting on the surface, plus tides (elevations at the open boundaries and equilibrium forcing at the surface). Four baseline runs were performed for Hurricane Ike: (a) the 2-D model forced by tides, winds, and pressures (called 2D-A); (b) the 2-D model forced by tides, winds, pressures, and waves (called 2D-W); (c) the 3-D model forced by tides, winds, and pressures (called 3D-A); and (d) the 3-D model forced by tides, winds, pressures, and waves (called 3D-W). For the 2D-A and 2D-W runs, the Manning

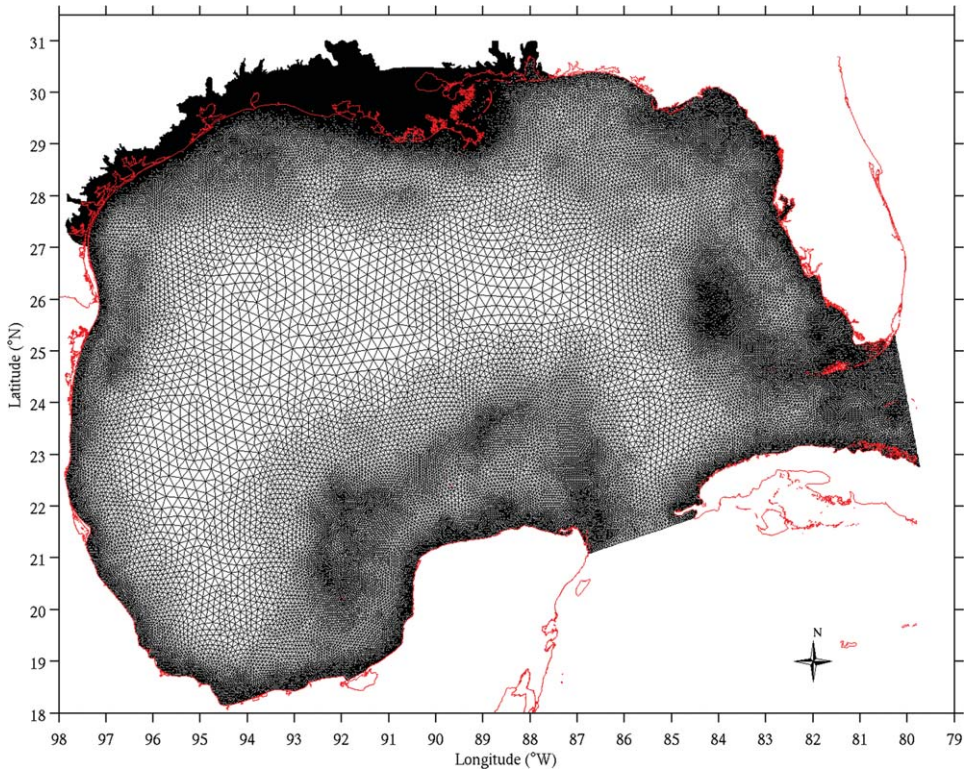

Figure 3. The unstructured triangular grid used in present model study. The red line is the coastline. The resolution varies from 100 m to 30 km.

coefficients were spatially varying with minimum value of 0.012 and maximum value of 0.2. For the 3D-A and 3D-W runs, the bottom roughness was held constant at 0.6 cm. The model runs all began at 1200 UTC on 31 July 2008, and ended at 0000 UTC on 16 September 2008 (a total run duration of 48 days). The simulation end date corresponded to 3 days after Hurricane Ike made landfall on 13 September 2008. The time steps used in these model runs were 1 s for the external mode and 5 s for internal mode (of the 3-D model). These time steps were chosen to ensure both model stability and smooth flooding/drying transitions. All of the model runs were performed on the Ranger cluster, administrated by Texas Advanced Computing Center, University of Texas at Austin.

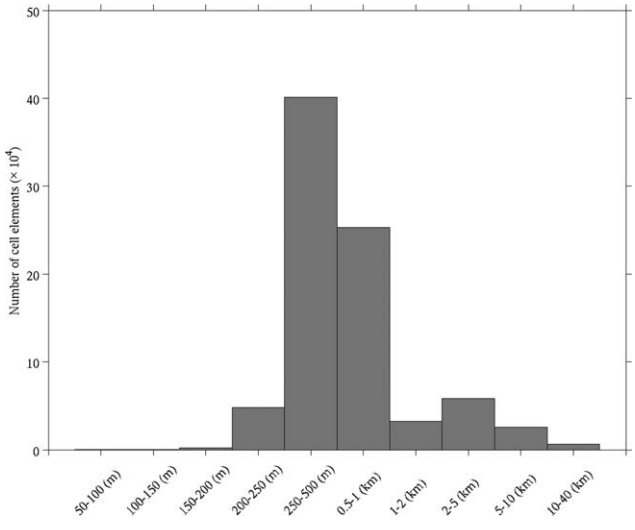

Figure 4. A histogram of the model grid cell dimensions.

4. 2-D and 3-D Hurricane Ike Storm Surge Simulations

[18] Over 800 observed water level and wave time series, or high water marks, were collected along the Gulf of Mexico coast coinciding with the Hurricane Ike landfall near Galveston Bay, TX. Time-series comparisons between model simulations performed as part of the U.S. IOOS Coastal and Ocean Modeling Testbed (R. A. Luettich et al., The U.S. IOOS Super-regional Coastal Ocean Modeling Testbed: Implementation and overview of findings, submitted to *Journal of Geophysical Research: Oceans*, 2013) may be viewed at http://www.sura.org/und/tropical-storms_130115/SURAIOOS_MAP_v3.htm. For our purposes here, we selected the three NOAA tide gauge stations [at Calcasieu Pass (Station No. 8768094), Sabine Pass (Station No. 8770570), and Galveston Pier (Station No. 8771510)] located to the north and east of the hurricane landfall point (see Figure 1), as examples for comparison with the simulations. Our discussions begin with the 2-D and 3-D coupled wave and surge simulations (2D-W and 3D-W, respectively) shown in Figure 5.

[19] Both simulations account for the observed surge levels reasonable well, but each with some subtle differences. In Calcasieu Pass, the 2D-W model simulation is in good agreement with the observation before 12 September 2008 when the sea level variation is mainly controlled by tides. As Hurricane Ike approaches landfall the 2D-W

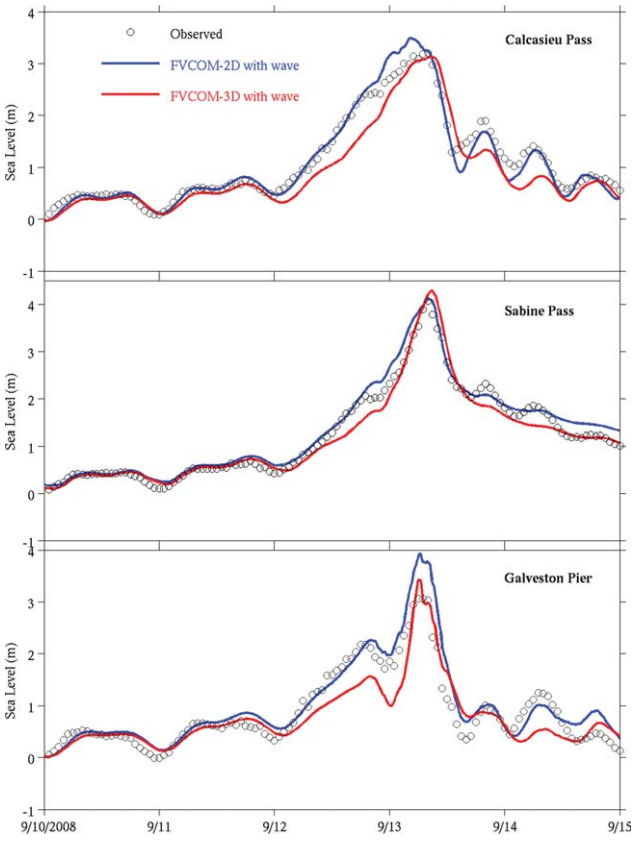

Figure 5. Time-series comparisons of observed (opened circles), 2D-W (blue) and 3D-W (red) simulated surges at (top) Calcasieu Pass, (middle) Sabine Pass, and (bottom) Galveston Pier NOAA tide gauged stations.

model simulation captures the initial rapid increase of sea level (i.e., forerunner) very closely, whereas the 3D-W does not respond so well. The 2D-W model simulation then peaks at 0430 UTC on 13 September 2008 with a storm surge of 3.5 m, about 3.5 h earlier and 0.3 m higher than observed. After landfall both the simulation and observation show sea levels rapidly decreasing from 3.5 to 0.9 m in 10 h, followed by a slower decrease along with tidal oscillations. In comparison with the 2D-W simulation, the 3D-W simulation underestimates the initial storm surge forerunner, but then peaks more closely with the observation at 0800 UTC on 13 September 2008 with a storm surge of 3.1 m, or about 0.1 m smaller than observed.

[20] At Sabine Pass, located closer to the point of landfall than Calcasieu Pass, both the 2D-W and 3D-W model simulations are in good agreement with the observation, both in storm surge amplitude and phase. As at Calcasieu Pass, the 3D-W also underestimates the magnitude of the forerunner.

[21] At Galveston Pier, located on the Ike track line (Figure 1), the 2D-W, while overestimating the observed storm surge, simulates the forerunner very well. The 3D-W simulation agrees better with the peak surge, but underestimates the forerunner. Both capture the phase equally well.

[22] It is generally recognized that wave radiation stress gradients tend to increase surge height by adding to the effect of wind stress [e.g., *Huang et al*., 2010; *Luettich and Westerink*, 1999]. To investigate the contribution made by wave coupling, we overlay the 2D-A and 3D-A simulations (forced by tides, wind stress, and atmospheric pressure only) onto the 2D-W and 3D-W simulations in Figure 6. As expected, the wave radiation stress adds incrementally to the storm surge without waves. Throughout the evolution of the surge, the wave radiation stress effect adds to the wind stress resulting in an increase in sea level, first through Ekman-geostrophic spin up (for the forerunner) and then downwind for the final shallow water surge. The contributions to the simulated surge heights by wave coupling are about 0.3 m to 0.4 m at these three stations regardless of the 2-D and 3-D formulations. This is consistent with the finding by *Huang et al*. [2010] for the hypothetical Ivan-like Hurricane simulation for the Tampa Bay region of Florida.

[23] Given the subtle differences between the 2-D and 3-D simulations, when compared with observations at three different coastal stations (Figures 5 and 6), what are the larger spatial scale differences in sea level set up and how might these be explained dynamically? For simplicity, the following analyses exclude wave effects. First consider the spatial distribution of surge height at different time steps in the evolution. Figure 7 shows the sea level distributions for the 2D-A (left) and 3D-A (right) simulation at 1800 UTC on 12 September 2008, and 0000 and 0600 UTC on 13

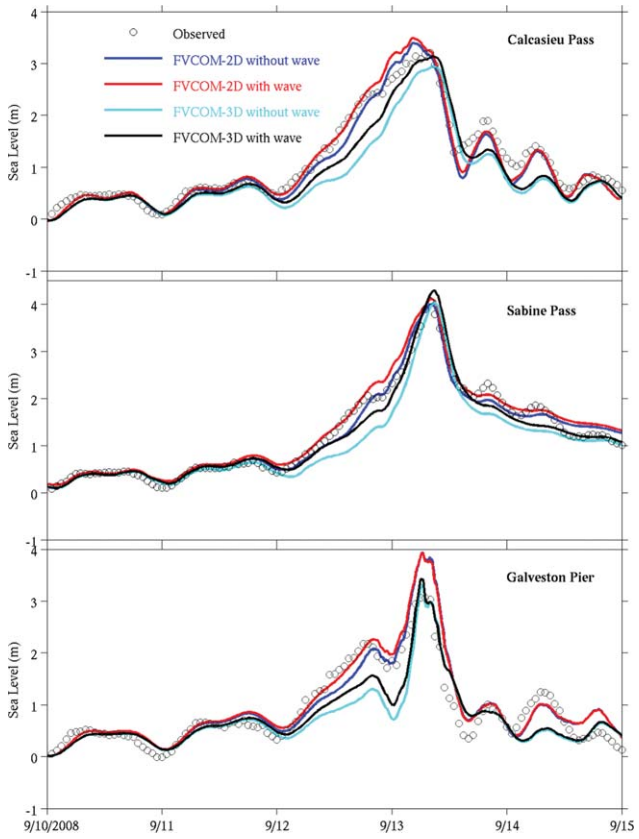

Figure 6. Time-series comparisons of observed (opened circles), 2D-A (blue), 2D-W (red), 3D-A (cyan), and 3D-W (black) simulated surges at (top) Calcasieu Pass, (middle) Sabine Pass, (bottom) and Galveston Pier NOAA tide gauged stations.

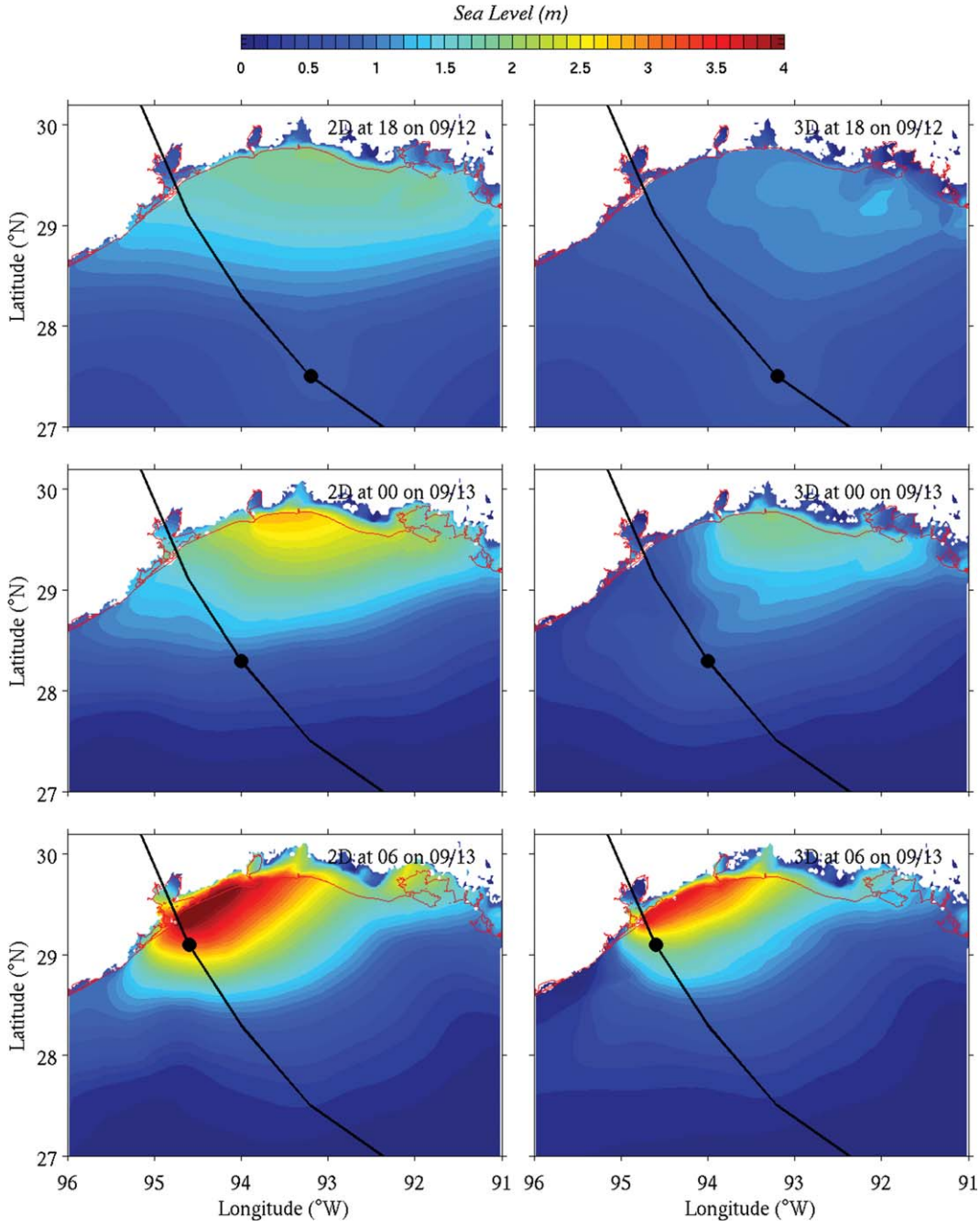

Figure 7. Evolution of sea level distributions at (top) 1800UTC on 9/12, (middle) 0000UTC on 9/13, and (bottom) 0600UTC on 9/13 for (left) 2D-A and (right) 3D-A simulations.

September 2008, that is, from 15 to 3 h before Hurricane Ike made landfall. These spatial maps show that the 2D-A surge exceeds the 3D-A surge everywhere. For either simulation, there is an initial forerunner attributed to an Ekman-geostrophic spin up to along shore wind stress during the time when the storm center is offshore and the winds are tending to be shore parallel near the coast (for instance, see *Weisberg et al*. [2000] for the coastal ocean response to a typical synoptic scale frontal passage and *Kennedy et al*. [2011] for a specific discussion on the Hurricane Ike forerunner). Six hours later, when the center of Ike was located at about 120 km southeast of the Galveston Bay, a combination of shore parallel and shore normal winds, increases the surge height and concentrates it more in space. Then at 0600 UTC on 13 September 2008, 3 h before landfall, the concentrated surge, due primarily to the shore normal winds, exceeds 4 m in the 2D-A simulation and 3.5 m in the 3D-A simulation.

[24] To arrive at an explanation for the differences in simulated sea level evolutions between 2D-A and 3D-A, we first consider the horizontal distributions of the 2D-A depth-averaged currents and 3D-A near bottom currents shown in Figure 8. Whereas the directions of the velocity vectors are similar in 2D-A and 3D-A (as determined by

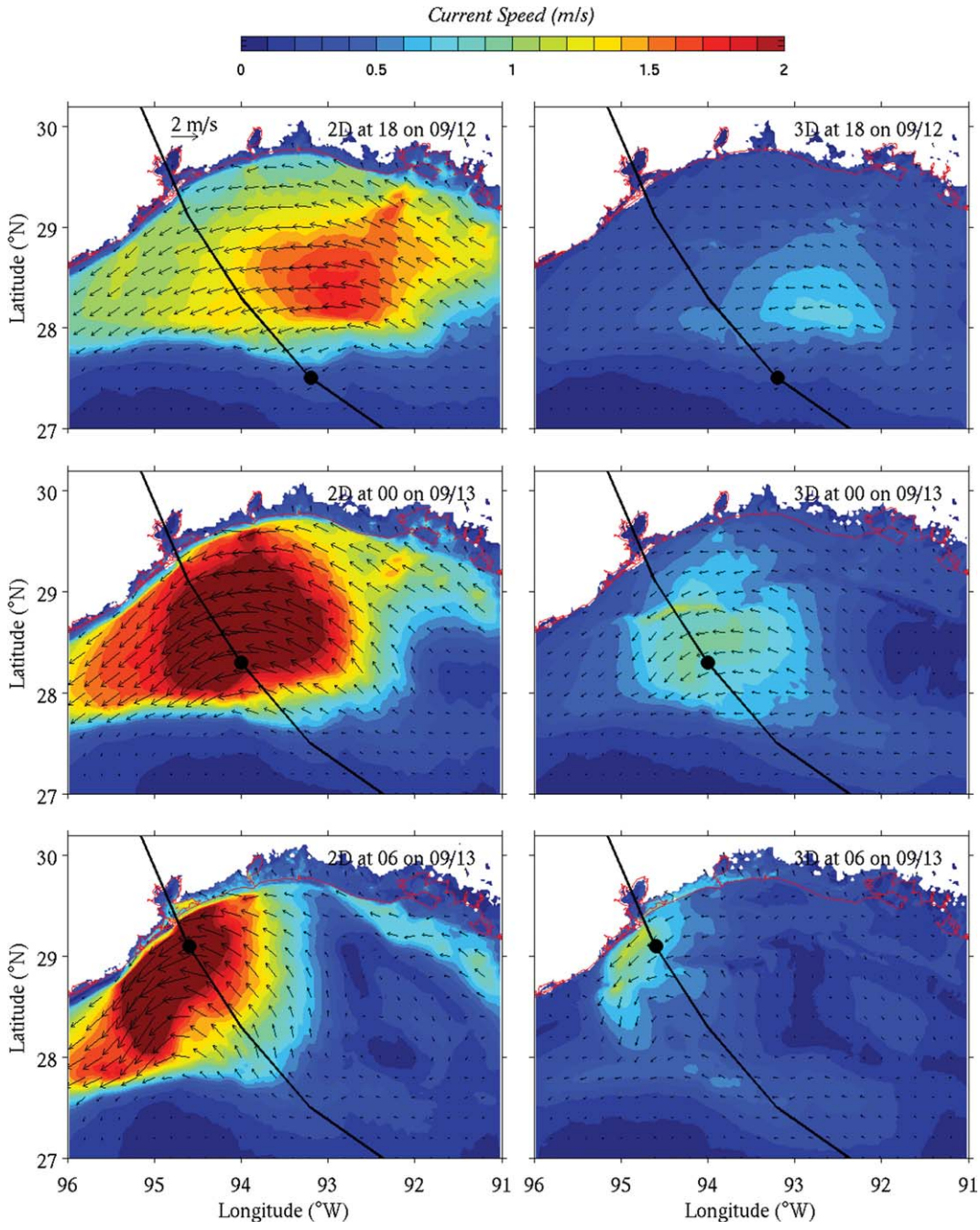

Figure 8. Evolution of near bottom current vector distributions at (top) 1800UTC on 9/12, (middle) 0000UTC on 9/13, and (bottom) 0600UTC on 9/13 for (left) 2D-A and (right) 3D-A simulations.

the wind stress directions), the magnitudes of the 2D-A simulated depth-averaged currents are much larger than the 3D-A simulated near bottom currents, particularly to the right of the storm track. Using equations (1)–(3), the bottom stresses corresponding to simulated current distributions of Figure 8 are shown in Figure 9. Because the bottom stress is proportional to the product of a bottom drag coefficient and the square of the current velocity, despite the 2D-A simulated depth-averaged current being much larger than the 3D-A simulated near bottom current, the 3D-A bottom stresses exceed the 2D-A bottom stresses because the 2D-A bottom drag coefficients are at least one order of magnitude smaller than the 3D-A bottom drag coefficients. Thus the reduced surge height for the 3D-A simulation, relative to the 2D-A simulation, is explained on the basis of the bottom stress being larger for the 3D-A simulation. This finding is reflected in the spatial distributions of vertically integrated pressure gradient force (Figure 10). With the primary balance for this being, the difference between the surface and bottom stresses, if the bottom stress for 3D-A is larger than for 2D-A, the vertically integrated pressure gradient force for 3D-A must be smaller than for 2D-A being that the surface wind stress is the same for both simulations. An immediate conclusion is that a

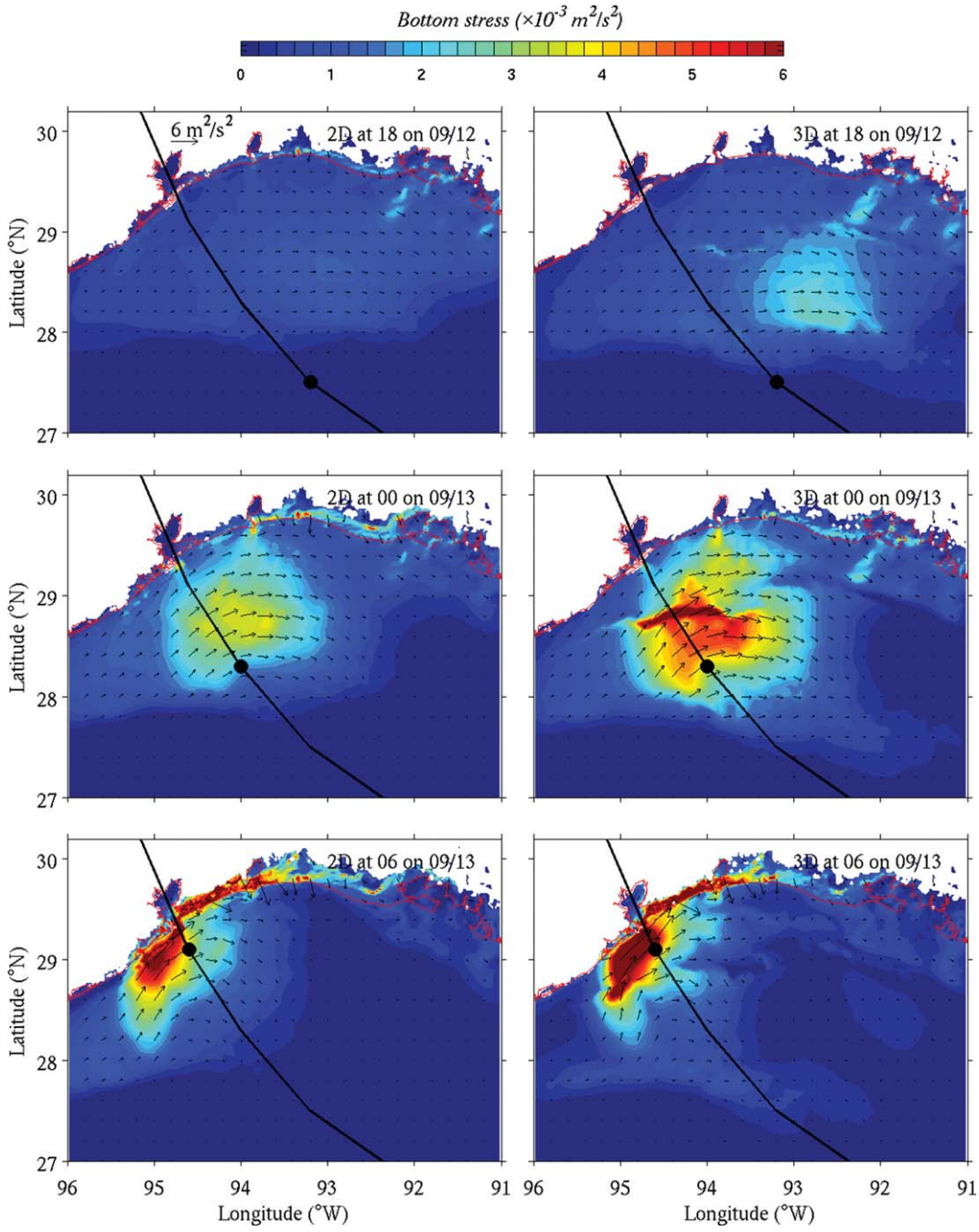

Figure 9. Evolution of bottom stress vector distributions at (top) 1800UTC on 9/12, (middle) 0000UTC on 9/13, and (bottom) 0600UTC on 9/13 for (left) 2D-A and (right) 3D-A simulations.

storm surge simulation is critically dependent on the parameterization of bottom friction.

[25] Further discussion on the lead terms in the vertically averaged momentum balance is made based on an across shelf section drawn seaward from Sabine Pass (Figure 1). Vector time-series evolutions for the wind stress minus the bottom stress ($\tau_w - \tau_b$) and the vertically averaged pressure gradient (PG), Coriolis (C), and local acceleration (LA) forces are shown in Figure 11. The left- and right-hand plots are for the 2D-A and the 3D-A simulations, respectively, and the temporal progressions from top to bottom are from 2200 UTC on 12 September 2008 to 0900 UTC on 13 September 2008. In each plot, the abscissa represents the distance offshore, with 0 corresponding to the seaward end of the transect, a total distance of 0.6^0 or about 66 km, from the shore line. Beginning at 2200 UTC on 12 September 2008, when Hurricane Ike is located offshore in deep water, we see that the momentum balance is primarily between the PG and the C forces for both the 2D-A and the 3D-A simulations, except at the coastal station where the bottom stress is large. As Ike approaches landfall a momentum balance transition occurs around 0300 UTC on 13 September 2008, such that by 0600 UTC on 13 September 2008, the primary balance is between $\tau_w - \tau_b$ and the PG

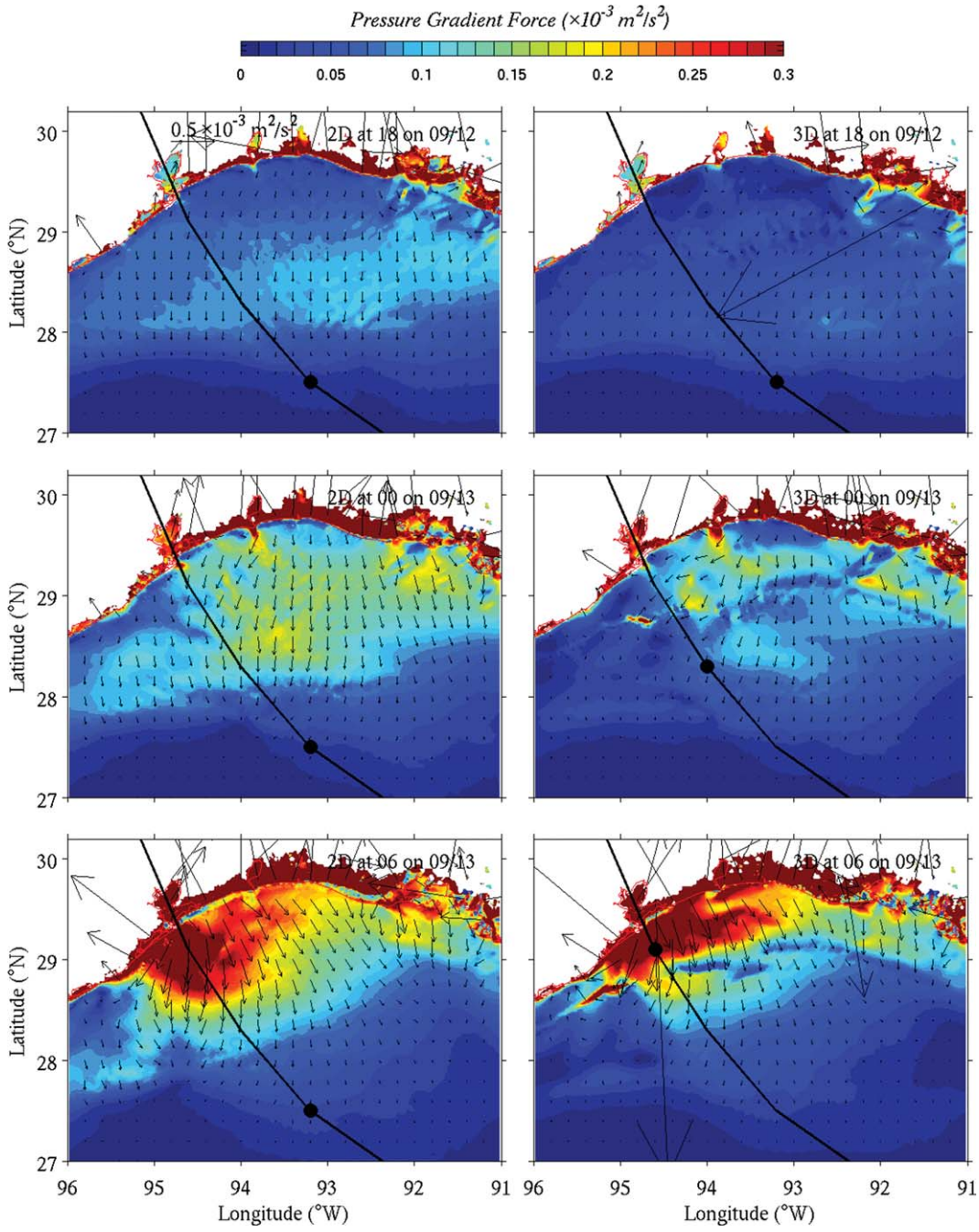

Figure 10. Evolution of pressure gradient forcing vector distributions at (top) 1800UTC on 9/12, (middle) 0000UTC on 9/13, and (bottom) 0600UTC on 9/13 for (left) 2D-A and (right) 3D-A simulations.

along the entire transect. The magnitudes of these lead terms further increase at 0900 UTC on 13 September 2008, when Ike makes landfall. At the coast at this time, and for both the 2D-A and the 3D-A simulations, the current flows offshore resulting in an onshore directed bottom friction force that adds constructively to wind stress.

[26] From the above momentum balance discussion, we see that the storm surge forerunner, observed when the storm center is still over the deep ocean, is the result of an Ekman-geostrophic spin-up response to along shelf winds, as regularly seen on continental shelves, even in response to the passage of synoptic scale weather fronts. The forerunner is then superseded by the actual storm surge (when the storm is over shallow, versus deep water) for which the PG force is balanced by $\tau_w - \tau_b$. Two points follow from these momentum analyses. First, being that the forerunner significantly affects coastal sea level, the model domain must be large enough to fully contain the storm while it is still at some distance offshore, that is, the model must account for the along shore wind-forced effects by Ekman geostrophic spin-up, either locally, or remotely and then propagated by continental shelf wave dynamics. Second, with the storm surge resulting from an imbalance between surface and bottom stresses the parameterization of these

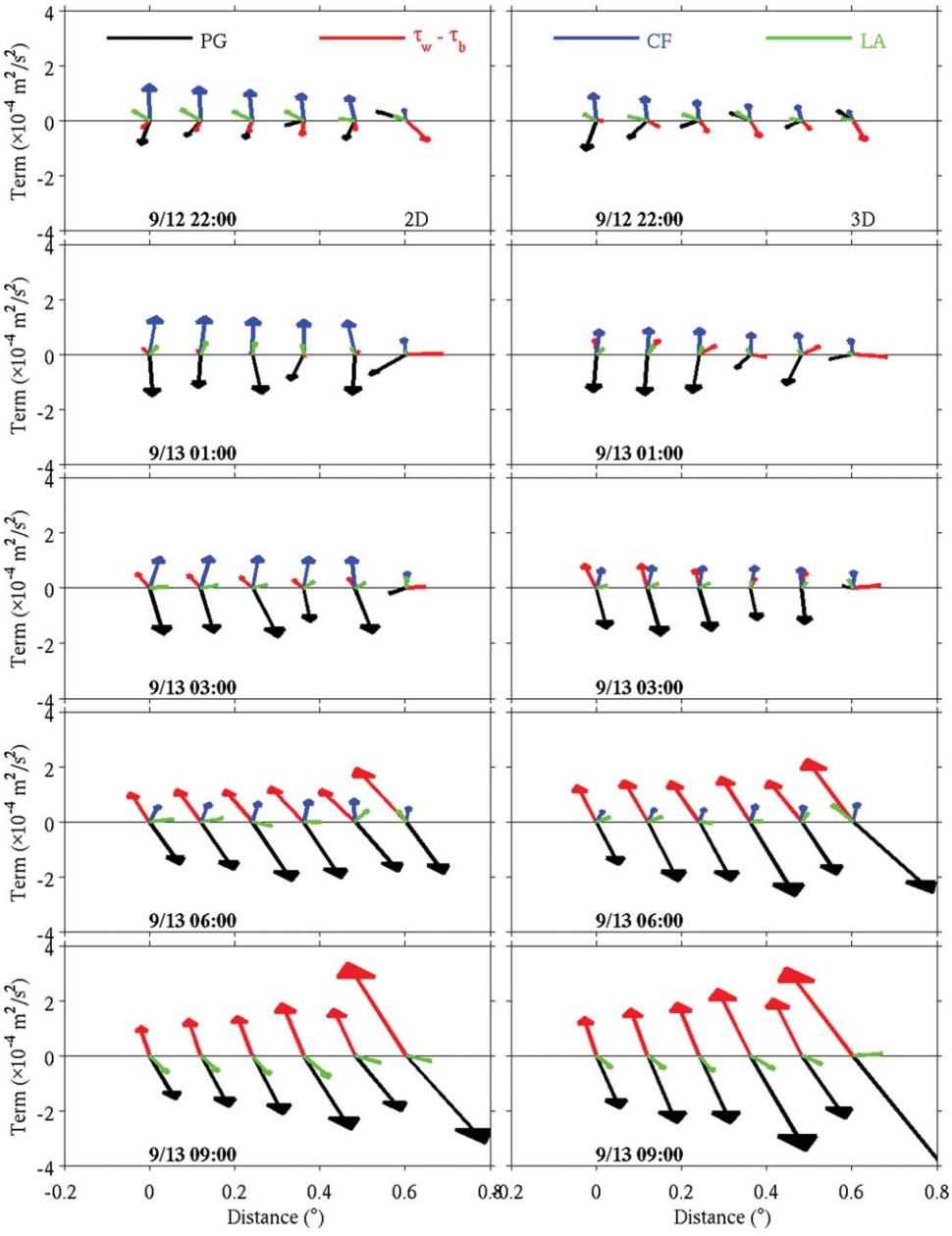

Figure 11. Evolution of momentum balance terms of pressure gradient (black), surface stress minus bottom stress (red), Coriolis force (blue), and local acceleration (green) on the selected across-shore section (shown in Figure 1) at (from top to bottom) 2200UTC on 9/12, 0100, 0300, 0600, and 0900UTC on 9/13 for (left) 2D-A and (right) 3D-A simulations.

stresses determine the magnitude of the surge. Uncertainties in both wind stress and bottom stress parameterizations are important for either 2-D or 3-D surge simulations, and comparisons between 2-D and 3-D simulations, each with the same wind stress parameterization, are critically determined by differences in their bottom stress parameterizations.

5. Effects of Bottom Drag Coefficient Parameterizations on Simulated Storm Surges

[27] Recall that the governing parameter for the bottom drag coefficient in the 2-D simulation is the Manning coefficient, whereas for the 3-D simulation, it is the bottom roughness. Three different scenarios are now investigated. The first considers 2-D simulations using two different Manning coefficient minimum values to ascertain the storm surge sensitivity to this parameter choice. The second considers a hybrid between 2-D and 3-D simulations (QUASI-2D) by using the same bottom roughness-determined drag coefficient, but with a log layer scaling for comparison with the full 3-D simulation, as in *Weisberg and Zheng* [2008]. The third considers a 3-D simulation with a drag coefficient derived from the 2-D Manning formulation.

[28] Two simulations are compared for the first scenario, both with spatially varying Manning's n, but each with different minimum values (0.012 as in 2D-A and 0.025 as now

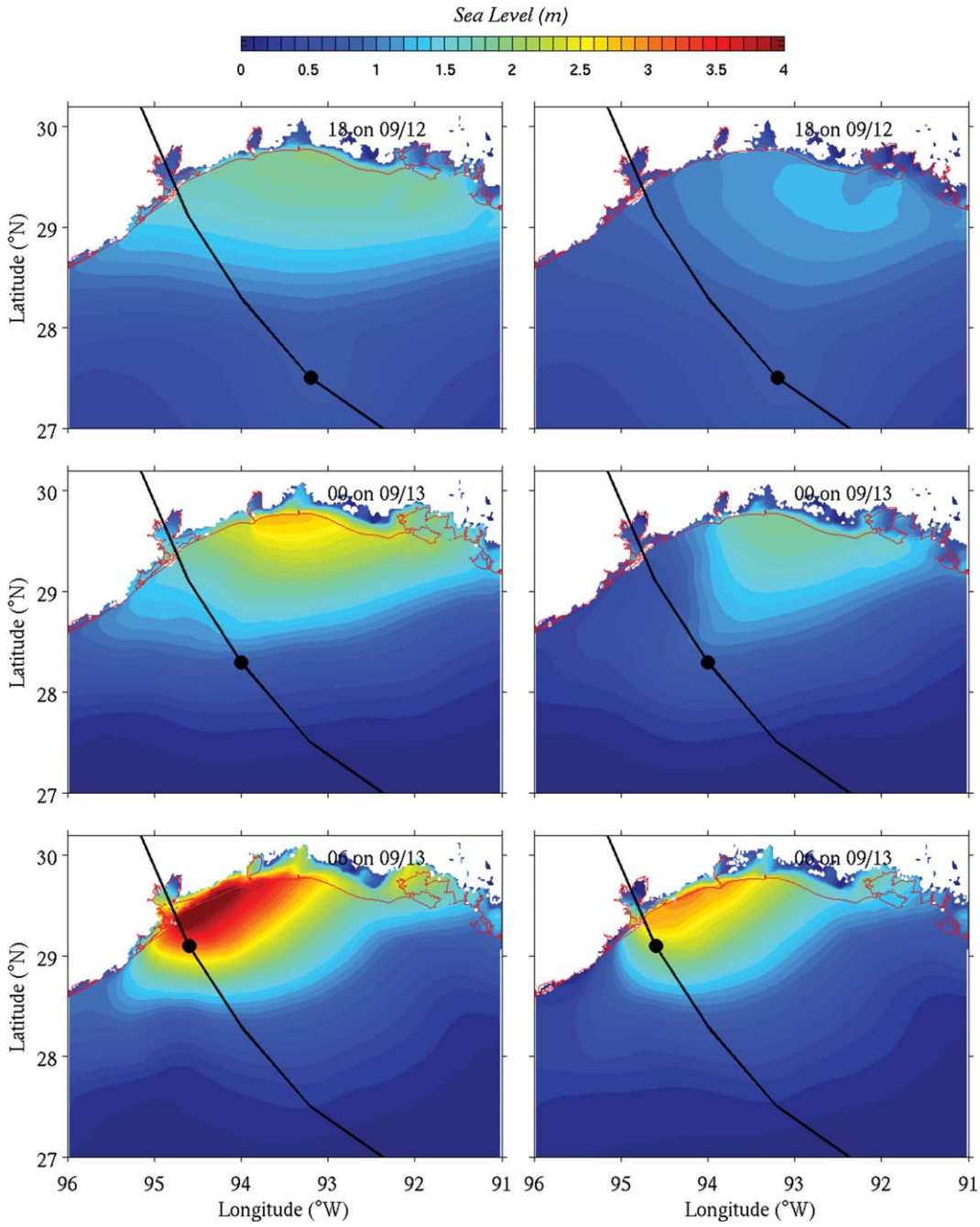

Figure 12. Evolution of sea level distributions at (top) 1800UTC on 9/12, (middle) 0000UTC on 9/13 and (bottom) 0600UTC on 9/13 for (left, minimum Manning coefficient value of 0.012) 2D-A and (right, minimum Manning coefficient value of 0.025) 2D-B simulations.

in 2D-B). Given that the bottom drag coefficient is proportional to the square of Manning coefficient (equation (2)), the bottom drag coefficient for 2D-B will be more than four times that of 2D-A in regions where minimum Manning's n values apply (which in this case is nearly the entire (preinundation) coastal ocean. The left- and right-hand plots of Figure 12 show the Hurricane Ike simulated sea level evolutions for cases 2D-A and 2D-B, respectively. Large differences in storm surge magnitude are observed throughout the evolution. At 1800 UTC on 12 September 2008, about 15 h before landfall, the 2D-A simulated forerunner is considerably higher than that for 2D-B (by >0.5 m). These magnitude differences increase as the storm approaches the coast such that at 0000 UTC on 13 September 2008, the 2D-A simulation exceeds that of 2D-B by > 0.8 m, and there is an overall shift in the spatial distribution of these two simulated surges. At 0600 UTC on 13 September 2008, 3 h before Ike makes landfall, the 2D-A and 2D-B simulated surges are about 4 m and 3 m, respectively. These surge differences correspond to PG force differences due to differences in $\tau_w - \tau_b$ deriving from the differences in the minimum Manning coefficient used in 2D-A and 2D-B.

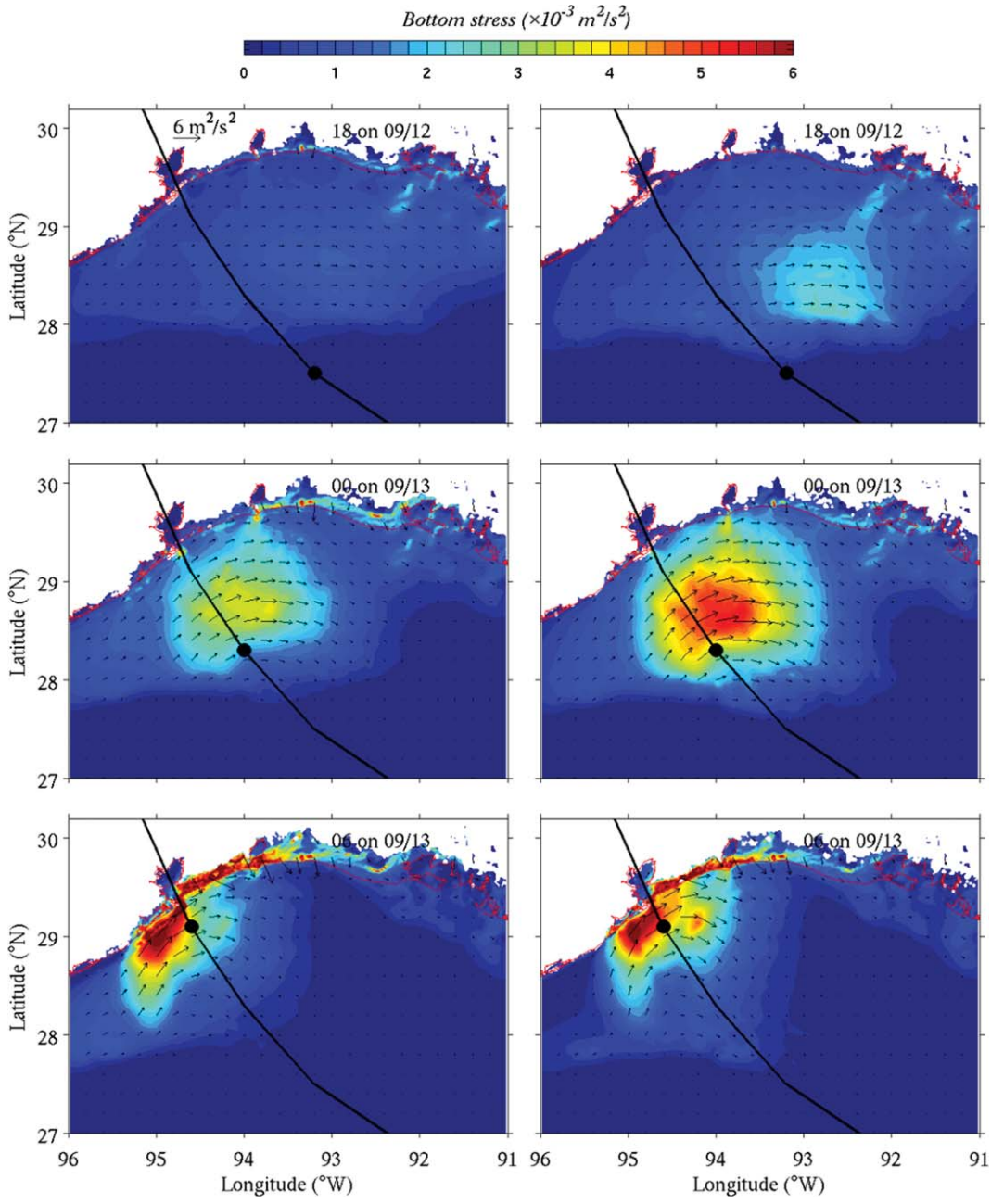

Figure 13. Evolution of bottom stress vector distributions at (top) 1800UTC on 9/12, (middle) 0000UTC on 9/13, and (bottom) 0600UTC on 9/13 for (left, minimum Manning coefficient value of 0.012) the 2D-A and (right, minimum Manning coefficient value of 0.025) the 2D-B simulations.

[29] Being that the surface wind stress is the same in 2D-A and 2D-B, of interest is how the minimum Manning coefficient translates to bottom stress, as shown in Figure 13, the left- and right-hand plots corresponding to 2D-A and 2D-B, respectively. At 1800 UTC on 12 September 2008, during the time of the forerunner, the 2D-B bottom stress magnitudes exceed those of 2D-A, implying smaller 2D-B currents and hence lesser geostrophic sea level set up along the coast (see momentum balances in Figure 11). The maximum bottom stresses, located at the right-hand side of the hurricane track, are 1.3×10^{-3} m^2/s^2 for 2D-A and 3.0×10^{-3} m^2/s^2 for 2D-B (top plots in Figure 13), respectively, and their corresponding along shore depth-averaged current speeds are 1.8 m/s for 2D-A and 1.4 m/s for 2D-B, respectively. At 0000 UTC on 13 September 2008, as the forerunner is transitioning to the actual storm surge, the maximum depth-averaged current speeds increase to 3 m/s for 2D-A and 1.7 m/s for 2D-B, and their corresponding bottom stresses are 3.7×10^{-3} m^2/s^2 for 2D-A and 5.5×10^{-3} m^2/s^2 for 2D-B (middle plots in Figure 13), respectively. At 0600 UTC on 13 September 2008, with Ike almost at landfall, the storm surge momentum balance is primarily between the PG force and $\tau_w - \tau_b$. With the bottom stress being of similar magnitude in both cases, the PG force is also of similar magnitude despite the surge height being larger for 2D-A than for 2D-B. The differences in

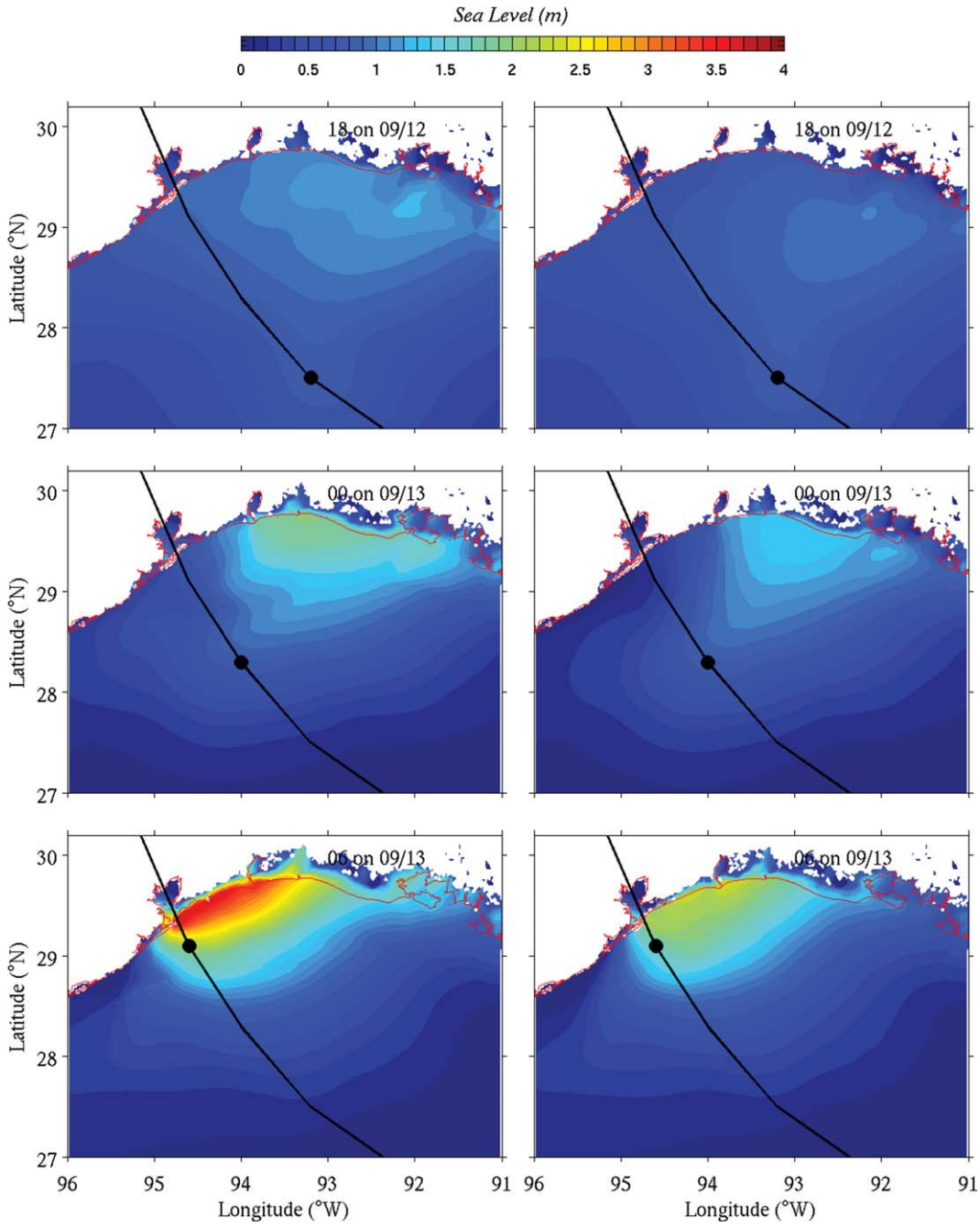

Figure 14. Evolution of sea level distributions at (top) 1800UTC on 9/12, (middle) 0000UTC on 9/13, and (bottom) 0600UTC on 9/13 for (left) 3D-A and (right) QUASI-2D simulations.

surge height are attributed mainly to the differences in the forerunner owing to the differences in minimum Manning coefficient applied.

[30] The second scenario, a hybrid between two and three dimensions, will be referred to as QUASI-2D. The idea is to compare 2-D and 3-D simulations using the same bottom drag coefficient. For this simulation, we approximate the 2-D case by using three terrain following σ-layers (-1.0, -0.9, 0.0) in the vertical along with a constant bottom roughness, $z_0 = 0.6$ cm, to produce the same bottom drag coefficient as for the previous 3D-A model simulation (equation (3)). This QUASI-2D approximation to a 2-D simulation using a 3-D model is the same as used by *Weisberg and Zheng* [2008] for their comparison between 2-D and 3-D simulations of hypothetical storm surges for Tampa Bay under Hurricane Ivan-like forcing. The bottom stress for the QUASI-2D simulation is determined using the upper layer velocity, which essentially is the depth-averaged velocity because the upper layer is 90% of the water column [e.g., see *Weisberg and Zheng*, 2008]. The left- and right-hand plots of Figure 14 show the sea level evolutions for the 3D-A and the QUASI-2D Hurricane Ike simulations, respectively. Similar to what was found by *Weisberg and Zheng* [2008], the QUASI-2D storm surge is

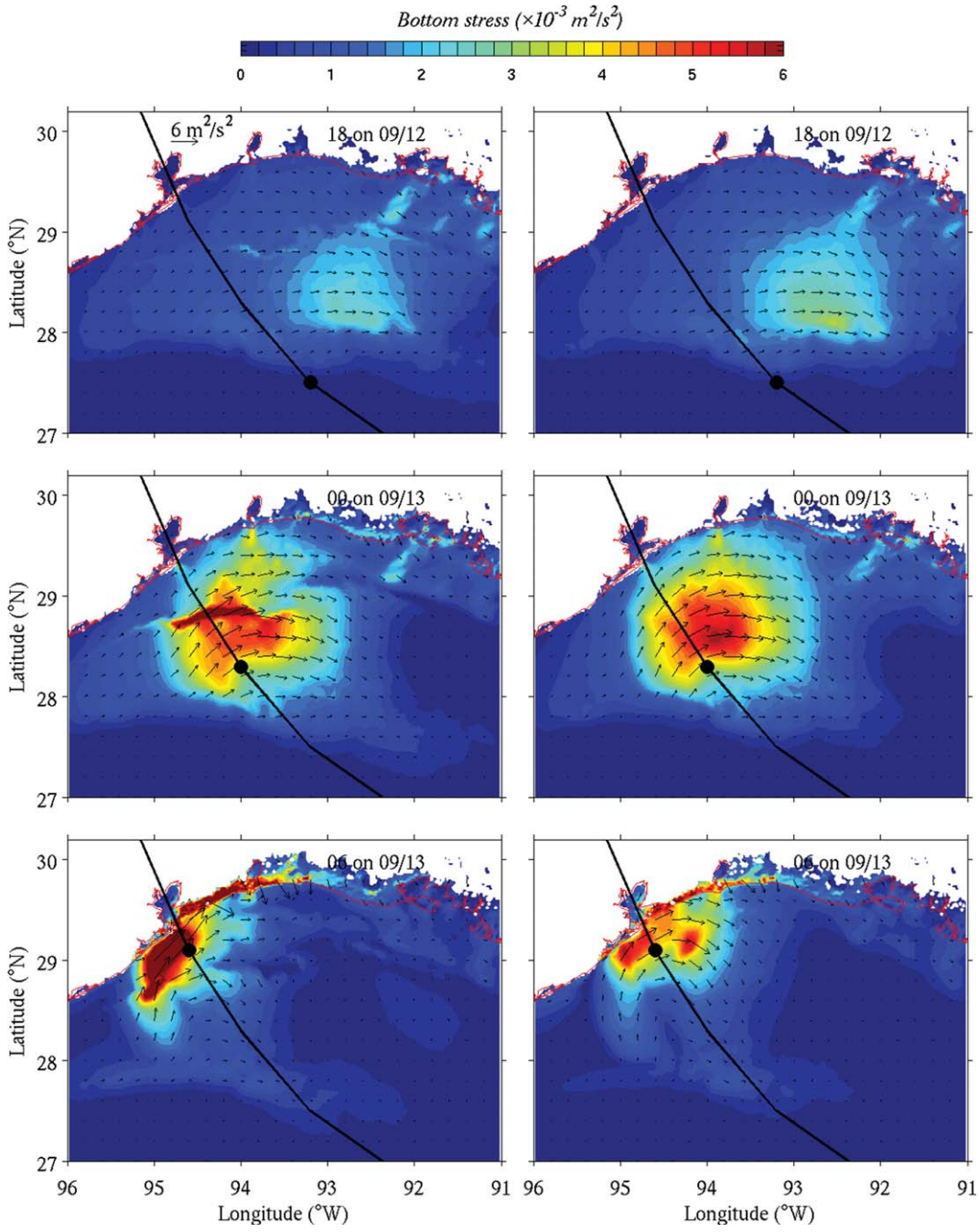

Figure 15. Evolution of bottom stress vector distributions at (top) 1800UTC on 9/12, (middle) 0000UTC on 9/13, and (bottom) 0600UTC on 9/13 for (left) 3D-A and (right) QUASI-2D simulations.

less than that for the 3D-A storm surge. For hurricane Ike this amounts to about 0.2–1 m over the event evolution. The explanation for these differences follows from the bottom stress evolutions (Figure 15). Owing to larger bottom stress and its spatial distribution (due to the depth-averaged velocity being larger than the near bottom velocity), the QUASI-2D storm surge evolves with smaller magnitude than that in the 3D-A simulation. From the two cases just considered (2D-A versus 2D-B with different minimum Manning coefficients and QUASI-2D versus 3D-A with the same drag coefficient but different velocities), it is clear that both the bottom stress formulations and the bottom drag coefficient parameterizations greatly impact the simulated storm surges.

[31] To bring the above argument full circle, it is necessary to consider 2-D and 3-D storm surge simulations made using the same bottom drag coefficient. We will refer to these simulations as 2D-A and 3D-B. To do this, we must convert the Manning coefficient used in a 2-D model to a bottom roughness used in a 3-D model. This is done by combining equations (2) and (3) to arrive at equation (4):

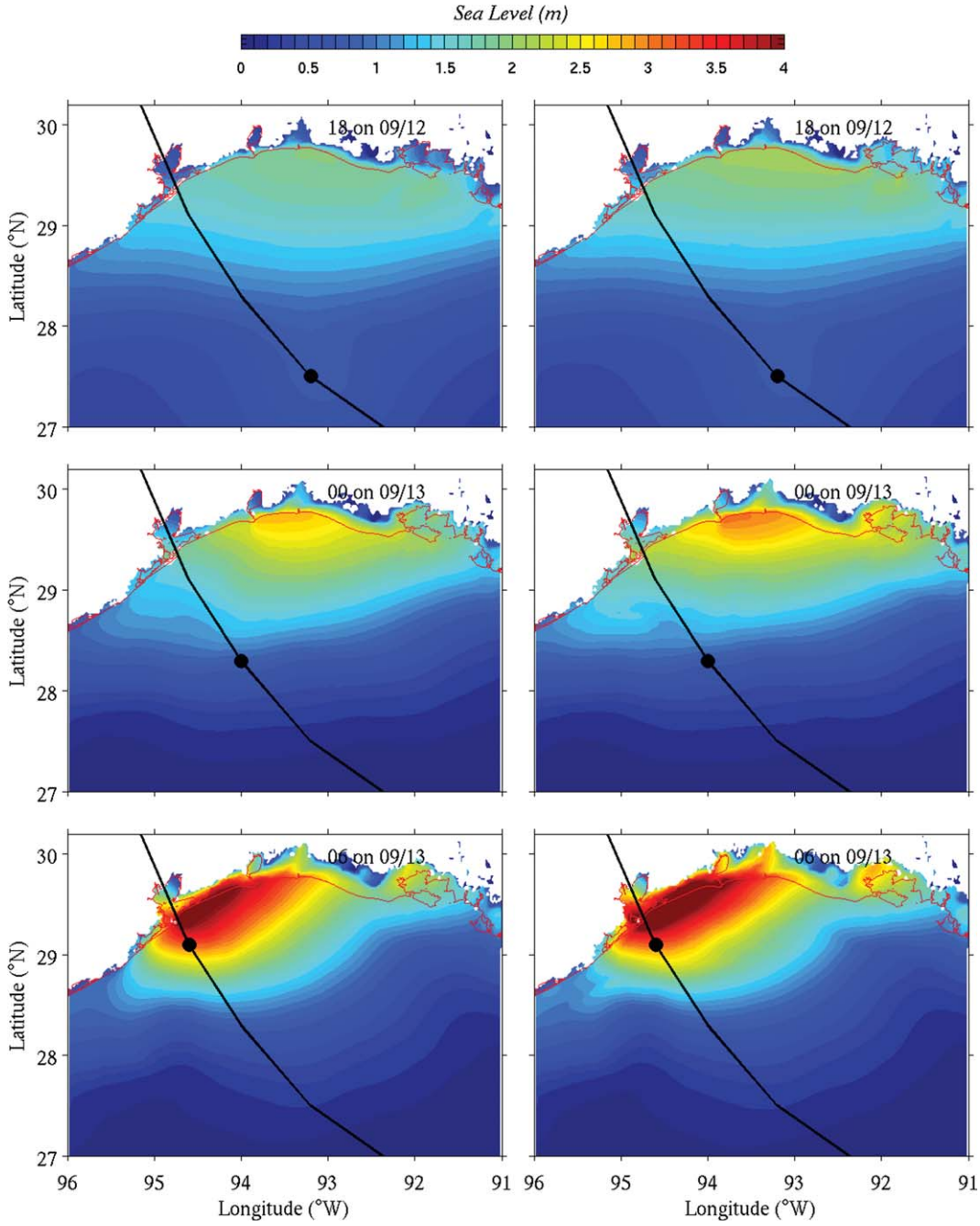

Figure 16. Evolution of sea level distributions at (top) 1800UTC on 9/12, (middle) 0000UTC on 9/13, and (bottom) 0600UTC on 9/13 for (left) 2D-A and (right) 3D-B simulations.

$$z_0 = 0.05 \cdot H \cdot \exp\left(-\frac{\kappa \cdot H^{1/6}}{\sqrt{g} \cdot n}\right) \tag{4}$$

a variation on a formula provided by *Bretschneider et al.* [1986], wherein the coefficient comes from the half thickness of the σ-layer closest to the bottom (0.05 in our application). By applying the spatially varying Manning's n from 2D-A in equation (4) to compute equivalent values of bottom roughness for use in equation (3), we obtain spatially varying 3-D bottom drag coefficients for use in 3D-B. In this way, both 2D-A and 3D-B have the same bottom drag coefficients. We note that while the depth dependent equation (4) provides a reasonable bottom roughness value in shallow water (less than ~50 m), the bottom roughness in the deeper water calculated from equation (4) tends to be very small.

[32] The left- and right-hand plots of Figure 16 show the sea level evolutions for the 2D-A and the 3D-B Hurricane Ike simulations, respectively. The spatial distribution patterns for sea level under both simulations are similar, although the 3D-B storm surge is somewhat higher than for 2D-A, especially in the bottom plot where the mature surge may be ~1.3 m higher. The explanation for these

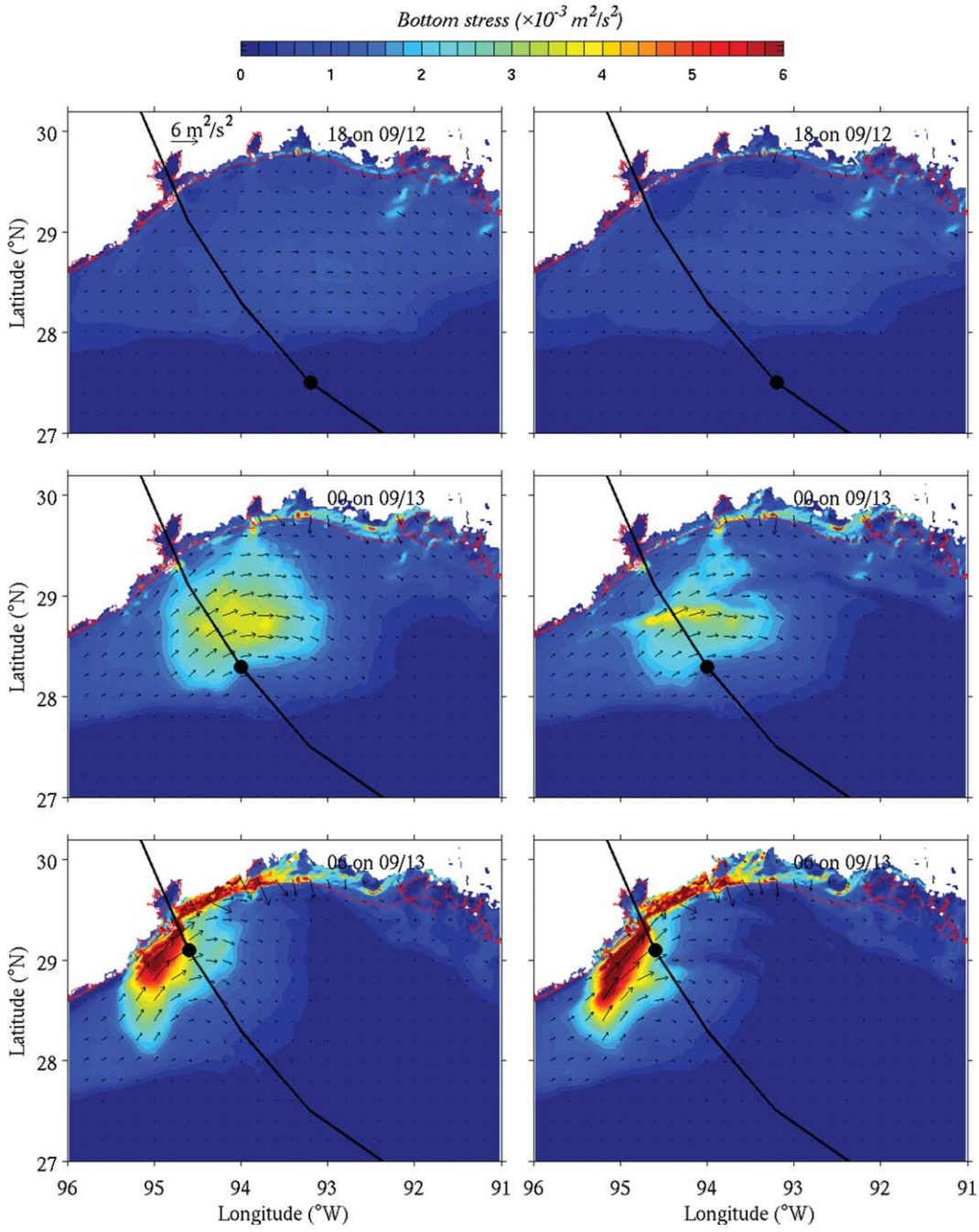

Figure 17. Evolution of bottom stress vector distributions at (top) 1800UTC on 9/12, (middle) 0000UTC on 9/13, and (bottom) 0600UTC on 9/13 for (left) 2D-A and (right) 3D-B simulations.

differences follows from the bottom stress evolutions (Figure 17). Since the bottom drag coefficients are the same for 2D-A and 3D-B, the magnitude of the bottom stress depends on the magnitude of the velocity used for the calculation. For 2D-A, the depth-averaged velocity may be larger than the near bottom velocity of 3D-B, especially on the right-hand side of the storm track, resulting in the bottom stress for the 2D-A exceeding that for 3D-B. Thus, even with the same bottom stress parameterization and formulation, the storm surge is also impacted by the differences in velocity under 2-D and 3-D formulations.

6. Discussions and Conclusions

[33] Storm surge simulations by numerical circulation models are dependent on the model domain and grid resolution, the quality of bathymetry and elevation data upon which the model grid is overlain and the wind and pressure fields used to force it. The parameterizations for friction and parameter values employed are also of critical importance.

[34] Our study of the Hurricane Ike storm surge investigated the simulation sensitivities to the model's vertical structure (2-D or 3-D) and the way in which the bottom stresses were parameterized in these formulations. Our use

of FVCOM, either in a 2-D or a 3-D formulation, followed from extensive testing and intermodel (ADCIRC, SELFE, SLOSH, and FVCOM) simulation comparisons (Kerr et al., submitted manuscript, 2013) within the framework of the Southeast University Research Association (SURA)-led, U.S. Integrated Ocean Observing System) IOOS Model Testbed Program. All of these models, with suitable parameter choices, achieved reasonable results when compared against each other and an extensive observational data base. Nevertheless, both model structure and parameter values, particularly for surface and bottom stress parameterizations, were important. For the Hurricane Ike storm surge simulation conducted here, we used the wind stress and pressure fields from Kerr et al. (submitted manuscript, 2013). With the model domain sufficiently large to avoid open boundary effects on the far field storm surge and the forcing products deemed to be the best presently available, we focused on 2-D and 3-D storm surge simulation comparisons relative to the bottom stress parameterizations employed.

[35] Four scenarios were considered. The first baseline scenario presented in section 4 compared a 2-D simulation with spatially varying Manning coefficient against a 3-D simulation with constant bottom roughness. In an attempt to explain the differences that were found we then investigated 2-D simulations with two different Manning coefficient minimum values, a hybrid between 2-D and 3-D simulations (QUASI-2D) by using the same bottom roughness-determined drag coefficient but with a log layer scaling for comparison with the full 3-D simulation, and a 2-D simulation with spatially varying Manning coefficient compared with a 3-D simulation for which the bottom drag coefficient was determined by a formal conversion of the Manning coefficient.

[36] The baseline scenario showed that reasonably good fidelity between observed and simulated storm surges may be achieved with either 2-D or 3-D model formulations when a range of Manning coefficients or a constant bottom roughness are used, respectively. However, when converting either the Manning coefficient or the bottom roughness to a bottom drag coefficient, the drag coefficient values for a 2-D formulation are about an order of magnitude smaller than those for a 3-D formulation. Vertical integration therefore changes the nature of the bottom stress calculation. Curiously, the baseline scenario showed better forerunner agreement with the 2-D model than with the 3-D model even though the surges were of similar magnitude.

[37] Diagnosing the momentum balances for the baseline scenario showed that the forerunner was primarily an Ekman-geostrophic spin-up response to alongshore wind stress, whereas the main surge was primarily a balance between the sea level gradient and the difference between the surface and bottom stresses. With the surface stress being the same for all scenario comparisons, their subtle differences derived from the bottom stress formulations and the parameters used to calculate bottom stress.

[38] The second scenario provided an example. Increasing the minimum value of the Manning coefficient from 0.012 to 0.025 reduced both the forerunner and the surge of the 2-D simulation, such that the 3-D (baseline) surge was larger than the 2-D (increased minimum Manning coefficient) surge (Figures 7 and 12).

[39] The third scenario confirmed the results of *Weisberg and Zheng* [2008] that, under the same bottom drag coefficient formulation, a 3-D simulation yielded a larger storm surge than a QUASI-2D simulation. The explanation is that the velocity magnitude used in calculating the bottom stress in QUASI-2D exceeded that in three dimensions and hence the bottom stress was larger. With larger bottom stress to counteract the surface stress, the sea level gradient was reduced from that of three dimensions.

[40] The fourth scenario was an attempt to bring the bottom stress calculations full circle back to the baseline scenario. Here we converted the spatially varying Manning coefficients that were used in two dimensions to spatially varying bottom roughness' for use in three dimensions by equating the two C_d formulations. Thus, the baseline 2-D and the fourth scenario 3-D simulations both used the same bottom drag coefficient. This resulted in very similar spatial evolutions of the forerunner and the surge. However, when converting to bottom roughness from the Manning coefficient in deep water, the bottom roughness values were as small as 10^{-7} m, which is physically unrealistic.

[41] The conclusions of this work are admittedly unsettled. First, whereas we can arrive at similar storm surge simulation results from either 2-D or 3-D model formulations, these results are critically dependent on the bottom stress formulations and the parameter values used when all else (model domains, grids, tide and surface forcing and bathymetry/topography) are the same. Given that a 2-D formulation is a simplification over a 3-D formulation, the bottom stress values tend to be smaller than those for three dimensions because larger horizontal velocities (by about a factor of three in our baseline case) necessitate smaller bottom drag coefficients (by about an order of magnitude in our baseline case). With empirically determined Manning coefficients, it is evident that a 2-D model is adequate for storm surge simulations. However, it remains unclear whether or not a Manning coefficient distribution for a given storm and location can be applied more generally for the purpose of predicting future event responses.

[42] Calibration also presents certain dilemmas that require explanation. For instance, our second scenario demonstrated that to simulate the forerunner correctly, the minimum value of the Manning coefficient had to be reduced below values previously considered in the literature [e.g., *Mattocks and Forbes*, 2008] to values generally associated with smooth, finished surfaces. But modeling the forerunner height more accurately resulted in overestimates (at some stations) of the surge itself. Thus balancing the need for forerunner accuracy relative to surge accuracy is a calibration issue. The baseline and the second scenarios used spatially variable Manning coefficient for two dimensions versus a constant bottom roughness for the 3-D baseline scenario. Choosing the spatial distributions of the Manning coefficient in a 2-D simulation, or the bottom roughness in a 3-D simulation, is a complicating factor, requiring a priori information on the compositions of the sea floor and the land to be inundated.

[43] When we compared 2-D and 3-D formulation results with all aspects kept as similar as possible (our QUASI-2D representation of two dimensions, enabling us to use the same bottom drag coefficient for two and three dimensions), the results of *Weisberg and Zheng* [2008] were again realized (that the 3-D surge height is larger than the

2-D surge height due to larger bottom stress in two dimensions). This result (following from a log layer scaling in the vertical) requires that an upper limit be placed on the drag coefficient, and this (as in two dimensions) requires calibration if applied more generally.

[44] The 2-D and 3-D results were most similar under the fourth scenario when the drag coefficients were equated through transformation of the Manning coefficient to bottom roughness. Unsetting, however, was the resultant miniscule value for bottom roughness in deep water.

[45] In conclusion, the primary limitations to storm surge hindcast or prediction are not the models themselves [FVCOM as used here, or ADvanced CIRculation ocean model (ADCIRC), Semi-implicit Eulerian-Lagrangian Finite-Element ocean model (SELFE), or any physically complete, high-enough resolution model], but the quantitative specifications of the parameterizations and parameter values that are used for specifying both the wind and bottom stresses. Here we circumvented the wind stress issue by using the sector-based analysis of *Dietrich et al*. [2011] that was adopted for surface forcing by the SURA IOOS Inundation Model Testbed. The intrinsic difference between 2-D and 3-D surge simulations is that by vertically integration, a 2-D model simplifies the vertical structure by eliminating the vertical distribution of turbulence and the nature of the surface and bottom boundary layers. However, such simplification requires its own calibration for bottom stress (spatially varying Manning coefficients). If calibration for individual storms and locations may be eliminated then a 2-D model is the most straight-forward and efficient approach to storm surge simulation.

[46] Given these conclusions it may be useful to distinguish between storm surge scenario projections and real-time predictions. Projections without time limitations (such as flood plain determinations for evacuation guidance and insurance rate maps) might benefit from an ensemble approach that uses both 2-D and 3-D models, each being run over a reasonable parameter set, to provide a range of expectation. Real-time prediction, on the other hand, necessitates rapid implementation of a surge model with the recognition that the answer will be critically dependent on the parameters chosen. To narrow the range of parameterizations and the parameter values employed for storm surge modeling in either 2-D or 3-D formulation, there remains a need for experimental guidance on the parameterizations and the parameter values associated with both the surface and the bottom stresses under severe wind conditions.

[47] **Acknowledgments.** This project was supported by NOAA via the U.S. IOOS Office (Award Numbers: NA10NOS0120063 and NA11NOS0120141) and was managed by the Southeastern Universities Research Association. Support for Zheng, Weisberg, and Huang was also derived from a grant from the Florida Catastrophic Storm Risk Management Center administered at the Florida State University, subaward number RO1270. This work used the Extreme Science and Engineering Discovery Environment (XSEDE), which is supported by National Science Foundation grant number OCI-1053575.

References

Bretschneider, C. L., H. J. Krock, E. Nakazaki, and F. M. Casciano (1986), Roughness of typical Hawaiian terrain for tsunami run-up calculations: A users manual, J.K.K. Look Laboratory report, Univ. of Hawaii, Honolulu, Hawaii.

Bunya, S., et al. (2010), A high-resolution coupled riverine flow, tide, wind, wind wave, and storm surge model for Southern Louisiana and Mississippi. Part I: Model development and validation, *Mon. Weather Rev.*, *138*, 345–377.

Chen, C. S., H. D. Liu, and R. C. Beardsley (2003), An unstructured, finite-volume, three-dimensional, primitive equation ocean model: Application to coastal ocean and estuaries, *J. Atmos. Oceanic Technol.*, *20*, 159–186.

Chen, C. S., Q. Xu, R. Houghton, and R. C. Beardsley (2008a), A model-dye comparison experiment in the tidal mixing front zone on the southern flank of Georges Bank, *J. Geophys. Res.*, *113*, C02005, doi:10.1029/2007jc004106.

Chen, C.S., J. Qi, C. Li, R.C. Beardsley, H. Lin, R. Walker, and K. Gates (2008b), Complexity of the flooding/drying process in an estuarine tidal-creek salt-marsh system: an application of FVCOM, *J. Geophys. Res.*, *113*, C07052, doi:10.1029/2007jc004328.

Chen, C. S., G. Gao, J. Qi, A. Proshutinsky, R. C. Beardsley, Z. Kowalik, H. Lin, and G. W. Cowles (2009), A new high-resolution unstructured-grid finite-volume Arctic Ocean model (AO-FVCOM): An application for tidal studies, *J. Geophys. Res.*, *114*, C08017, doi:10.1029/2008jc004941.

Dietrich, J. C., et al. (2011), Hurricane Gustav (2008) waves and storm surge: Hindcast, synoptic analysis and validation in Southern Louisiana, *Mon. Weather Rev.*, *139*, 2488–2522, doi:10.1175/2011MWR3611.1.

Feddersen, F., E. L. Gallagher, R. T. Guza, and S. Elgar (2003), The drag coefficient, bottom roughness, and wave-breaking in the nearshore. *Coastal Eng.*, *48*, 189–195.

Galperin, B., L. H. Kantha, S. Hasid, and A. Rosati (1988), A quasi-equilibrium turbulent energy model for geophysical flows, *J. Atmos. Sci.*, *45*, 55–62.

Hagy, J. D., J. C. Lehrter, and M. C. Murrell (2006), Effects of hurricane Ivan on water quality in Pensacola Bay, Florida, *Estuaries Coasts*, *29*, 919–925.

Holland, G. J. (1980), An analytic model of the wind and pressure profiles in hurricanes, *Mon. Weather Rev.*, *108*, 1212–1218.

Huang, Y., R. H. Weisberg, and L. Zheng (2010), Coupling of surge and waves for an Ivan-like hurricane impacting the Tampa Bay, Florida region, *J. Geophys. Res.*, *115*, C12009, doi:10.1029/2009JC006090.

Kennedy, A. B., U. Gravois, B. C. Zachry, J. J. Westerink, M. E. Hope, J. C. Dietrich, M. D. Powell, A. T. Cox, R. A. Luettich, and R. G. Dean (2011), Origin of the hurricane Ike forerunner surge, *Geophys. Res. Lett.*, *38*, L08608, doi:10.1029/2011GL047090.

Luettich, R. A., and J. J. Westerink (1999), Implementation of the wave radiation stress gradient as a forcing for the ADCIRC hydrodynamic model: Upgrades and documentation for ADCIRC version 34.12, contract report, 9 pp., Dep. of the Army, U.S. Army Corps of Eng., Waterw. Exp. Stn., Vicksburg, Miss.

Mattocks, C., and C. Forbes (2008), A real-time, event-triggered storm surge forecasting system for the state of North Carolina, *Ocean Modell.*, *25*, 95–119, doi:10.1016/j.ocemod.2008.06.008.

Mellor, G. L. and T. Yamada (1982), Development of a turbulence closure model for geophysical fluid problems, *Rev. Geophys.*, *20*, 851–875.

Orton, P., N. Georgas, A. Blumberg, and J. Pullen, (2012), Detailed modeling of recent severe storm tides in estuaries of the New York City region, *J. Geophys. Res.*, *117*, C09030, doi:10.1029/2012JC008220.

Rego, J. L., and C. Li (2010), Storm surge propagation in Galveston Bay during Hurricane Ike, *J. Mar. Syst.*, *82*, 265–279, doi:10.1016/j.jmarsys.2010.06.001.

Sallenger, A. H., H. F. Stockdon, L. Fauver, M. Hansen, D. Thompson, C. W. Wright, and J. Lillycrop (2006), Hurricane 2004: An overview of their characteristics and coastal change, *Estuaries Coasts*, *29*, 880–888.

Smagorinsky, J. (1963), General circulation experiments with primitive equations. I. The basic experiment, *Mon. Weather Rev.*, *91*, 99–164.

Weisberg, R. H., and L.Y. Zheng (2006a), A simulation of the hurricane Charley storm surge and its breach of North Captiva Island, *Fla. Sci.*, *69*, 152–165.

Weisberg, R. H. and L. Y. Zheng (2006b), A finite volume coastal ocean model simulation of the tide, buoyancy, and wind-driven circulation of Tampa Bay, *J. Geophys. Res.*, *111*, C01005, doi:10.1029/2005JC003067.

Weisberg, R. H., and L. Y. Zheng (2006c), Hurricane storm surge simulations for Tampa Bay, *Estuaries Coasts*, *29*, 899–913.

Weisberg, R. H. and L. Y. Zheng (2008), Hurricane storm surge simulations comparing three-dimensional with two-dimensional formulations based on an Ivan-like storm over the Tampa Bay, Florida region, *J. Geophys. Res.*, *113*, C12001, doi:10.1029/2008JC005115.

Weisberg, R. H., B. Black, and Z. Li (2000), An upwelling case study on Florida's west coast, *J. Geophys. Res.*, *105*, 11,459–11,469.

Weisberg, R. H., A. Barth, A. Alvera-Azcárate, and L. Y. Zheng (2009), A coordinated coastal ocean observing and modeling system for the west Florida continental shelf, *Harmful Algae*, *8*, 585–597, doi:10.1016/j.hal.2008.11.003.

Zheng, L. Y. and R. H. Weisberg (2010), Rookery Bay and Naples Bay circulation simulations: Applications to tides and fresh water inflow regulation. *Ecol. Modell.*, *221*, 986–996, doi:10.1016/j.ecolmodel.2009.01.024.

Zheng, L. Y. and R. H. Weisberg (2012), Modeling the west Florida coastal ocean by downscaling from the deep ocean, across the continental shelf and into the estuaries, *Ocean Modell.*, *48*, 10–29, doi:10.1016/j.ocemod.2012.02.002.

Zheng, L. Y., C. S. Chen, and H. D. Liu (2003), A modeling study of the Satilla River estuary, Georgia. I: flooding-drying process and water exchange over the salt marsh-estuary-shelf complex, *Estuaries*, *26*, 651–669.

Zijlema, M. (2010), Computation of wind-wave spectra in coastal waters with SWAN on unstructured grids, *Coastal Eng.*, *57*, 267–277.